Analysis of Information from the Installed Dynamic Line Rating (DLR) Systems, to Define a Deployment Plan Up to 2030

Beatriz Morales
Universidad Pontificia de Comillas
Madrid, Spain
beatrizmoralesmontoya@gmail.com

David Santacruz
Control systems department
i-DE Iberdrola
Bilbao, Spain
dspe@iberdrola.es

Matteo Troncia
Instituto de Investigación Tecnológica (IIT)
Universidad Pontificia de Comillas
Madrid, Spain
mtroncia@comillas.edu

***Abstract*— This document is a final master thesis, that has been carried out in collaboration with i-DE, Redes Eléctricas Inteligentes, the Distribution System Operator of Iberdrola's group. It consists of a statistical analysis of the information from the Dynamic Line Rating (DLR) testing systems already installed in some lines as a pilot project. DLR enables the optimization of existing line capacity based on weather conditions, and the primary objective of its implementation at Iberdrola is to enhance grid flexibility through reconfiguration. This study analyses and evaluates different DLR technologies, the impact of the weather variables and other parameters such as altitude, different standards for the calculation of the rating, DLR equipment, challenges with its deployment and future approaches. It is done with the ultimate purpose of defining recommendations for the 2030 deployment of this technology for Iberdrola group.**

Keywords—Dynamic Line Rating, Smart grids, flexibility

I. INTRODUCTION

Nowadays, energy is not only indispensable in our lives but also a key factor in development. In the past, energy was extracted from non-renewable sources like coal, natural gas, and oil, emitting greenhouse gases into the atmosphere when burned. The visible effects of climate change, such as rising temperatures, continuous heatwaves, and extreme weather events, have heightened society's concern about combating climate change. This is evident in the commitments made by countries, particularly in the EU, to reduce fossil fuel consumption and improve energy efficiency, as demonstrated by the Paris Agreement's goal of reducing emissions by at least 55% compared to 1990 [1].

To achieve these ambitious targets and accommodate the growing demand for energy, there has been a revolution in power systems. This new paradigm involves increasing the use of renewable energy sources, promoting self-consumption, integrating distributed generators, adopting electric vehicles, and electrifying the economy in general terms [2]. However, this transition from traditional power systems to one that integrates these new components presents challenges in both operation and network planning.

The integration of variable renewable sources poses previously unseen scenarios in transmission lines, such as reverse power flow. As an example, in Spain, the Spanish Transmission System Operator (REE) projects that 50% of the energy generated by 2023 will come from renewables [3]. This shift presents multiple technical and social challenges that need to be addressed, including the current network's capacity not being adequately prepared for the increased integration of renewables.

From the perspective of integrating Distributed Energy Resources (DERs), they need to be connected to the distribution grid, whereas in the past, renewables were typically connected to the transmission grid. This shift requires distribution companies to develop additional control mechanisms, essentially taking on the role of a Distribution System Operator (DSO), which is equivalent to the Transmission System Operator (TSO) but at the distribution level. In other words, they become a system operator rather than just a distributor.

To optimally integrate renewables and harness their full potential, increasing the transmission and distribution capacity of the grid is essential. This can be achieved by implementing new infrastructure, elevating voltage levels, utilizing low-loss or high-capacity conductors, modifying tower designs, and adopting dynamic management strategies [4]. While constructing new lines may seem like a straightforward solution, is not the more effective as its complexity, time-consuming, and cost, make it unsuitable for rapid network expansion [5]. Furthermore, the traditional solution of repowering the network to increase power capacity through equipment replacement is not sufficient to address the network's expansion, connection, and flexibility needs [6]. As a result, it raises the necessity of exploring alternative solutions beyond the traditional approach.

In response to the challenges posed by traditional power grids, smart grids, also known as intelligent grids, have emerged as a revolutionary solution. These types of grids utilize advanced technology and real-time data to improve grid management and optimize the existing network. Advances in control and automation of the power system have driven this transformation [7].

Until now, systems operators have managed the network using a static limit for the maximum current that the network can carry [8]. This limit is a single rating for the whole year that remains unchanged or at most two different ratings for summer and winter. To set these limits, the worst-case conditions are considered: no wind and the highest temperature. This conservative approach is known as Static Line Rating (SLR). Iberdrola has also been using this approach in its lines. It is intended to always operate the grid safely, but the problem is that almost always results in underutilization of the grid's true capacity [9].

The advancement of the traditional Static Line Rating (SLR) is the Dynamic Line Rating (DLR). As mentioned above, SLR is limited to considering only the worst conditions. In contrast, DLR takes into account real-time weather conditions such as ambient temperature, wind speed, wind direction and solar radiation as well as line-specific characteristics such as load, ground clearance, conductor sag, conductor voltage and conductor temperature [20]. Providing a dynamic and precise evaluation of a transmission line's ampacity, which is the maximum current it can carry safely in real-time.

The integration of DLR through applications such as Optimum Power Flow (OPF) in smart grids enables the optimization of network capacity while maximizing the utilization of existing infrastructure. Numerous studies illustrate the successful optimization of line ratings, such as the case presented in [10] within the German power system, [11] in the Australian power system, and [8], which indicates that an enhancement in static rates can be accomplished approximately 85% of the time. Additionally, various studies showcase how DLR can facilitate the integration of renewables [4],[12],[13]. DLR stands as a pivotal innovation within the smart grid framework, enabling real-time data utilization to enhance decision-making and more efficient management of the power system.

Iberdrola is also interested in this approach. In fact, a few years ago, Iberdrola installed DLR test equipment from two different suppliers in order to study and analyse the data for real deployment in the future. This capacity increase would allow this company to avoid blind investments in new lines by optimising the existing infrastructure, results to be a more cost-effective strategy. This project main objective is to analyse the data from the pilot DTR systems installed by the two different suppliers, with the future prospect of using the calculated ratings as input data for OPF calculations, necessitating the examination of variables like periodicity and safety coefficients.

The analysis is divided in two parts. The first part is based on a sensitivity analysis on parameters values modified artificially. These parameters are wind speed, wind direction, temperature, roughness, altitude above the sea level, absorptivity and emissivity coefficients. The aim of this analysis is to see how the different variables impact in the final result of the ampacity using the three different standards: IEEE, CIGRE 601 and CIGRE 207.

The second part involves analysing the data from the pilot equipment provided by the two distinct suppliers. Additionally, to facilitate comparison, data from the nearest meteorological station to the line is also incorporated, sourced from Open-meteo. The objective is to study the reliability of these systems, the validity of the weather parameters they used as input variables and the verification of their ampacity calculation. Furthermore, it seeks to study the utilization of safety coefficients, potential simplifications in calculation, the frequency of rating updates, and whether the installation of a sensor is necessary or if a predictive estimation suffices.

With the extracted results, recommendations are given for when Iberdrola plans the future deployment of this technology. The paper is structured as follows: Section II and Section III give an overview of the benefits and challenges of implementing DLR respectively. Section IV explains the different methods to calculate the rating. Section V compares the two different standards IEEE and CIGRE. Section VI exposes the case study. Finally, Section VII and Section VIII, give the results and conclusions of the analysis.

II. Benefits

There are multiple papers that explain in detail the benefits of implementing DLR in the power systems [14], [15], [16] and [17]. Next, a summary is provided for the most important ones.

- **Improved Grid Operations and Reliability:** DLR enhances grid flexibility, allowing for higher currents during emergencies, leveraging the thermal inertia of conductors. This provides additional system adaptability and ensures reliable power delivery for both base and peak loading. DLR technology contributes to more cost-effective power generation dispatch and aids in system planning by forecasting power-carrying capacity [16].
- **Reduced Need for Operator Intervention:** DLR along with OPF, reduces the need for manual intervention by providing real-time thermal rating information, automating decision-making processes, and optimizing grid operation.
- **Reduced Congestion on Power Lines:** As there is an increased capacity of the lines, there is a reduction in congestion.
- **Reduced Curtailment of Variable Renewable Energy (VRE):** There is a positive correlation between wind production and transmission capacity potentially available from overhead lines. As wind generation increases, the enhanced cooling effect on overhead conductors allows for greater transmission capacity. This alignment enables more wind energy to be transmitted during higher wind periods,

reducing generation curtailments and optimizing resource utilization.

- **Facilitated Rapid Access to Renewable Energy:** DLR accelerates the integration of distributed energy resources, streamlining the integration of variable renewable energy (VRE) sources like wind and solar. This facilitates quicker access to clean energy, saving time and resources that would otherwise be required for the construction of new transmission lines.
- **Enhanced Utilization of Distributed Generation:** DLR reduces curtailment of distributed generation production, that in most cases is renewable, in maximizing the use of locally generated power.
- **Reduced Capital Costs and Investments:** Optimized asset utilization through DLR minimizes the need for new infrastructure investments as new lines, leading to cost savings and improved cost efficiency of power lines. Considering alternative methods such as DLR allows to optimise investments, avoiding those that are unnecessary.
- **Financial Benefits to Consumers and Market Participants:** By increasing transmission capacity and optimizing power flow, the cost of connecting generators to the grid is reduced, particularly facilitating the entry of renewable energy sources. The higher presence of renewables in the market dispatch would lead to a decrease in energy costs, ultimately benefiting consumers. Furthermore, if DLR is employed with forecasting, it facilitates more efficient day-ahead and real-time markets by providing more accurate estimations of expected transmission capacity. This enables more effective power trading activities.
- **Reduced Carbon Footprint:** The reduction of the carbon footprint is not only attributed to allowing greater consumption of distributed energy, often from renewable sources. It is also due to the reduction of line extensions, which further contributes to minimising this footprint.

III. Challenges

To enable the successful implementation of this new technology, several key factors are essential, which could be categorized as challenges to overcome [16], [14].

- **Data collection and digitization of the grid:** Challenges arise in collecting data, which can be achieved through sensors or meteorological sources like Agencia Estatal de Meteorología (AEMET). The latter approach has a drawback as measurements are not collected on-site directly from the line, but rather obtained from the nearest weather station, introducing a margin of error. Conversely, sensor-based data collection on the line presents its own set of challenges, including high installation and maintenance costs, susceptibility to interference, and uncertainties associated with measurements. Additionally, robust communication and control systems are essential for effective DLR operation.
- **Thermal aging:** In the implementation of DLR, the focus on maximizing the thermal capacity of transmission lines can accelerate the process of thermal aging in conductors. By operating cables closer to their thermal limits, higher temperatures are generated in the conductors, which can expedite the degradation of their properties over time.
- **Reliability and security:** Ensuring the reliability and security of DLR technology requires thorough validation and verification of its used technologies. Uncertainties can stem from sources like measurement and model inaccuracies. Detecting accurate weather data is critical and missed data due to equipment failures poses another issue. Sensor calibration is necessary for precision. The broader security analysis of the power grid might be insufficient when integrating DLR, demanding careful evaluation. There is a financial risk of exceeding line limits, which can be costly. Moreover, if a line breaks, its operation halts until replacement, incurring substantial expenses.
- **Integration into system operation:** At first glance, for system operators, there might appear to be only drawbacks, as implementing DLR could potentially compromise the security and reliability of the system. Consequently, they might be reluctant to adopt it. Therefore, incentives must be provided for such technologies (indeed, they are already recognized as retributable investments) to encourage system operators to overcome their reservations and install a DLR system.
- **Variability of ampacity:** Dispatching based on highly variable real-time ratings is impractical due to constraints in generation dispatch and load response. To address this, strategies like averaging ratings over time, constraining rating ranges, and clustering dynamic values into finite states can be employed to minimize rating variability and enhance the feasibility of DLR integration.
- **Application Development:** DLR's potential is limited without a dedicated application to safely implement its capacity enhancements within the power system. Therefore, a secure application as Optimal Power Flow (OPF) is essential to ensure the safe application of increased capacity.
- **Difficulty to calculate the economic benefit:** While the substantial reliability advantages of implementing DLR are acknowledged, accurately quantifying the economic value poses a significant hurdle [14].
- **Calculation algorithms:** Standards from organizations such as the International Council on Large Electric Systems (CIGRE) [18] and the Institute of Electrical and Electronics Engineers (IEEE) [19] are commonly used for calculating ampacity in overhead conductors. It is important to note that uncertainties exist in these calculations, particularly when temperatures approach the conductor's limit. The accuracy of these calculations relies on input data, including the physical properties of the conductor, geographical

information about the line's location, and atmospheric variables [16].

- **Regulation:** Traditionally, regulations based on investment costs, such as rate of return and cost-plus regulation, have been prevalent for making grid operation and investment decisions. However, these approaches have limitations and may not effectively encourage efficient utilization of existing infrastructure. To address these limitations, regulators have introduced regulations focusing on operational expenditures (OPEX) to incentivize transmission system operators (TSOs) to enhance operational practices and reduce the need for new physical infrastructure investments. These regulations incorporate incentives like rewards and penalties, motivating TSOs to achieve transmission capacity targets set by regulators and allowing them to share in the "extra profit" if these targets are exceeded. Embracing such OPEX-based solutions, like DLR, promotes innovative approaches to power system operation, reducing the need for capital expenditures (CAPEX) in new infrastructure.
- **Critical Spans identification:** The temperature of the conductor fluctuates along the line primarily due to variances in wind distribution. The ampacity of the transmission line is established based on the segment that experiences the least cooling effect, known as the critical span. On a transmission line, there may be multiple critical spans. As a result, pinpointing the locations and quantities of devices necessary to monitor these vital spans presents a challenge during the implementation of the DLR system [14].

IV. Methods for Calculating DLR

Two distinct methods for calculating DLR are available, they differ in the monitoring system used to collect the input variables for the calculation.

A. Direct Method

The line rating is calculated based on direct measurement power line characteristics such ground clearance, conductor sag, tension, and conductor temperature. Point sensors for direct conductor temperature offer insights from specific locations, potentially missing worst-case points. Conversely, conductor tension and sag monitoring systems provide a comprehensive view of weather conditions across the entire transmission line, allowing calculation based on average conductor temperature conditions.

B. Indirect Method

It uses the weather data as input to calculate the line rating. This data can be collected either from sensors installed in the line or from forecast meteorological source as AEMET. The ampacity calculation through weather variables is based on the basic heat balance equation, where the gained heat is equal to the lost heat. It also depends on ohmic losses, skin effect, conductor type and the geographical location. These factors can be categorised into two main groups: the physical properties of the conductor and the atmospheric conditions in which it operates. Various standards govern the calculation of ampacity using this approach, with the most prominent and relevant ones for this project being IEEE, CIGRE 207, and CIGRE 601 (an updated version of CIGRE 201).

In Table 1, it is outlined the advantages and disadvantages of each approach. The indirect method offers simplicity, cost-effectiveness, and reliability, requiring no sensor installation on the line itself. However, it may lack precision in representing worst-case conditions and introduces uncertainty in ampacity estimation due to indirect determination based on theoretical models. On the other hand, the direct method provides accurate measurements of physical quantities but involves field data analysis, calibration, and potential inaccuracies in certain scenarios.

Table 1: Advantages and Disadvantages of the direct and indirect methods.

Method	*Advantages*	*Disadvantages*
Indirect Method	-Simplicity: No need for sensors on the line.	-Precision Limitations: May not accurately represent worst conditions.
	-Cost-Effectiveness: Low installation and maintenance cost.	-Uncertainty: As it is an indirect estimation, the line temperature and ampacity determined indirectly, introducing potential errors.
	-Reliability: Highly reliable, minimal for special calibrations.	-Limited Environmental Data: Meteorological stations provide data only for specific areas, without local variations.
	-Investigative Potential: Allows investigation of estimated temperature reasons.	- Environmental Variability: Wind speed and direction variations affected by terrain and obstacles.
	- Multi-Purpose Suitability: Enables short-term and long-term load capacity forecasts.	
Direct method	-Precise Measurement: Provides accurate measurement of physical quantities (e.g., temperature, sag).	- Calibration and Analysis: Requires field data analysis and calibration for accurate results.
		- Limited Representative Data: Data related to the measured span may not represent average conditions along the entire line.
		- Inaccuracies: Large errors may arise for lightly loaded lines or small conductor temperature rises over ambient.
		-Maintenance Challenges: High maintenance costs and potential line interruption requirements.

Considering the trade-offs, the indirect method, particularly using weather stations, emerges as the best solution due to its crosschecking capabilities and ability to forecast load capacity in both short- and long-term perspectives. The accuracy of local weather forecasts becomes pivotal in ensuring the success of this approach [23]. This is the method that this study analyses.

V. Comparation between CIGRE and IEEE Standards

The calculated temperatures are very similar between the two standards. Furthermore, according to multiple studies, the temperature error (|Tmeasured – Tcalculated|) is less than 5°C 85% of the time [20]. Numerous studies have conducted comparisons between these standards, including [21], [22], [23], [20] and [10]. Below, there is a summary of the main differences in their calculations.

A. Conductor heating

As the magnetic and the corona heating effects are neglected in both standards, solar and joule effect are the two remains effects that affect the temperature of the conductor.

The conductor's temperature-dependent DC resistance is calculated in a similar way in both standards, the only difference is that IEEE standard does not include an AC to DC current conversion, whereas the CIGRE model includes.

The solar heating depends on many variables as the coefficient of absorption of the conductor, line's orientation and latitude, the hour and day of the year, and atmospheric clarity. It is necessary to calculate the position of the sun and the solar intensity. The solar intensity, direct and diffuse can be measured by a sensor. However, the installation and upkeep of such sensors come with substantial expenses. Given that the sensor's impact on the final result is not particularly significant, both standards offer an alternative calculation method to estimate global solar radiation.

Due to the cyclic magnetic flux produced by the spiralling current around the steel core, ACSR conductors become magnetically heated. The amount of aluminium encasing the steel core and current flow are two elements that affect heating. The skin effect, magnetic heating, and losses related to ACSR conductors are all taken into account by an approximative correction equation built into the CIGRE model. The IEEE standard, in contrast, ignores both magnetic losses and the skin effect.

B. Conductor cooling

The cooling of the conductor is produced by the convective and radiative effects. Both standards use the same calculation for the radiative cooling, considering the gradient of the temperature between the conductor surface and the ambient, the diameter of the conductor and the emissivity coefficient.

The major difference between these two standards lies in the approach to calculating convective cooling. CIGRE employs Morgan correlations relying on the Nusselt number, while IEEE utilizes McAdams correlations grounded in the Reynolds number [20]. Furthermore, the CIGRE standard accounts for the conductor's surface roughness, which the IEEE standard does not consider. This inclusion intensifies the impact of forced convection on the conductor. Consequently, the IEEE standard is generally viewed as a more conservative approach to convection cooling calculation.

VI. Case Study

This project focuses on an overhead transmission line, which has been selected because both suppliers have their equipment installed on it, enabling the comparison. The line is located between Rocamora and Carrús, situated in the municipality of Elche, Spain. The static line rating is 200 A, and it operates at 132 kV. On this line, Supplier 2 has installed two vibration sensors, while Supplier 1 has deployed five sets of sensors. The subsequent sections explain in more detail the equipment installed by the two different suppliers; both uses the indirect method to calculate the ampacity.

A. Supplier 1

Supplier 1's equipment is comprised of sensors for each atmospheric variable to be measured: wind speed, wind direction, solar radiation, and ambient temperature. These sensors are positioned on the towers supporting the power lines. To calculate ampacity using atmospheric variables, Supplier 1 employs the CIGRE 207 standard. It provides minute-by-minute ratings.

B. Supplier 2

Supplier 2's equipment exclusively employs a cable vibration sensor, which is located in the line, to derive effective wind speed and sag values. The remaining meteorological data is obtained through a weather subscription service, utilizing a Weather API to access external variables. The concept of "effective" wind refers to the wind speed equivalent at a 90-degree angle to the cable, which has the most substantial impact. The supplier provides line ratings each five-minute.

The following table summarizes the main characteristics of each supplier.

Table 2: Comparison between the two Suppliers.

Aspect	Supplier 1	Supplier 2
Input data collection	Wind speed, wind direction, temperature, solar radiation sensors in line towers	Cable vibration sensor on the line for the wind, the rest of the variables taken from a weather source
Standard	CIGRE 207 standard	Unknown
Wind Consideration	Real wind direction	Calculates "effective" wind at 90º
Rating Frequency	Minute by minute	Every 5 minutes

The data used for the first part of the analysis is showed in Table 3. From these data, the parameter under investigation is varied in each sensitivity analysis.

Table 3: Parameters used for the sensitivity analysis.

Temperature (°C)	26
Wind speed (m/s)	10
Wind direction (°)	90
Solar radiation (W/m²)	566
Day	11/06/2023
Hour	12:00:00
Roughness	0.04

For the second part of the analysis uses the historical data from the systems of the providers for the period from March 8, 2023, to June 30, 2023. Additionally, data of this specific period is collected from a weather source, Open-Meteo [24], in order to compare it with the data from the suppliers.

VII. Results

A. *Analysis of the Standards*

- Impact of the wind speed

When considering Rs=0.04 and varying the wind speed, Figure 1, there is little difference between the IEEE and CIGRE standards, with the maximum difference being 37.21 A between IEEE and CIGRE 601 at a wind speed of 0.4 m/s. The average difference between IEEE and CIGRE 601 is 13.78 A.

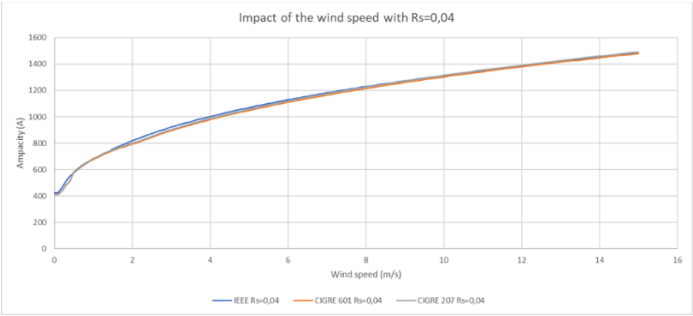

Figure 1: Wind speed analysis Rs=0.04.

For Rs=0.08, at low wind speeds, the results from both standards are similar as Figure 2 shows. Nonetheless, around 3 m/s wind speed, the difference between IEEE and CIGRE starts to increase significantly, reaching a maximum difference of 267.35 A at a wind speed of 15 m/s. The average difference is 121.26 A between IEEE and CIGRE 601, much more than when Rs=0.04. This is due to the fact that with Rs>0.05, the CIGRE standards use higher coefficients to calculate the Nusselt Number.

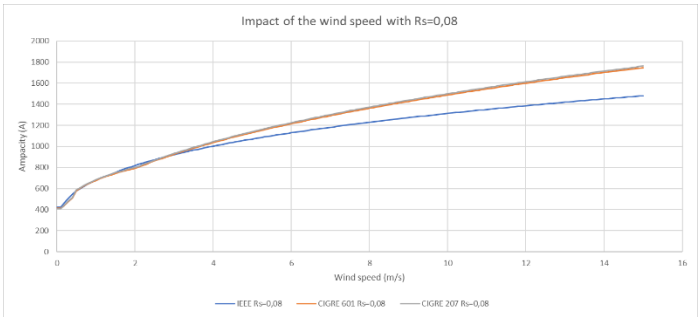

Figure 2: Wind speed analysis Rs=0.08.

- Impact of the wind direction

If the variable being varied is the wind direction over the transmission line, the result is Figure 3.

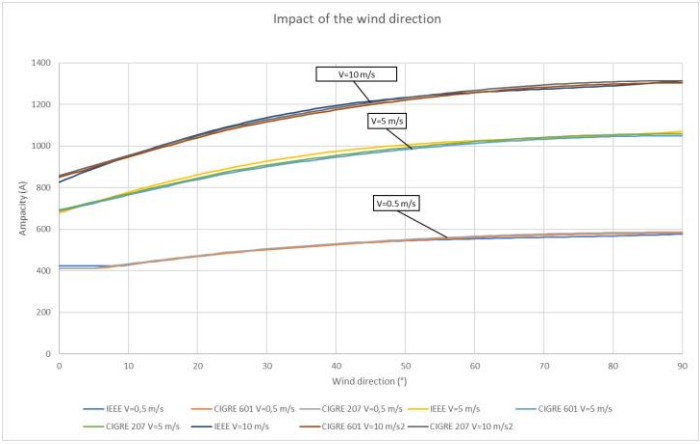

Figure 3: Wind direction analysis.

The results show minimal changes among the different standards as the wind angle varies from 0 to 90 degrees. The average difference between IEEE and CIGRE 601 is 5.29 A, 16.30 A, and 10.91 A at wind speeds of 0.5 m/s, 5 m/s, and 10 m/s, respectively.

The differences between the standards can be attributed to the way they consider the wind angle. In the CIGRE standard, the impact of the wind angle on ampacity depends on whether the wind angle is greater than 24 degrees or not. Conversely, the IEEE standard adopts a different approach to handle the wind attack angle. Instead of using a fixed threshold like CIGRE, the IEEE standard continually adjusts the constant multiplier based on the wind attack angle. This dynamic approach means that even slight variations in the wind direction can result in variations in the calculated ampacity, making it a more sensitive method to account for wind angle effects.

- Impact of the temperature

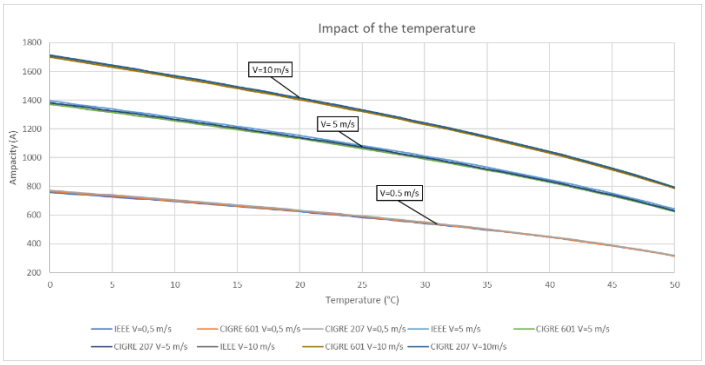

Figure 4: Temperature analysis.

The analysis reveals minimal variation among the standards when the ambient temperature is varied from 0ºC to 50ºC , with the average differences being 3.54 A, 21.18 A and 10.30 A at wind speeds of 0.5 m/s, 5 m/s, and 10 m/s, respectively. It is evident that higher temperatures result in lower ampacity values as Figure 4 shows. Both standards consider temperature as a crucial factor in the calculation of cooling convection, as lower temperatures allow for more cooling. Additionally, temperature significantly affects radiated heating, where heat is transferred

from higher to lower temperatures. Consequently, in colder ambient conditions, the cable is allowed to transfer more heat to the surroundings. Moreover, it is observed that at higher wind speeds, the impact of temperature becomes more pronounced, as indicated by the more defined envelope in the results.

- Impact of the altitude

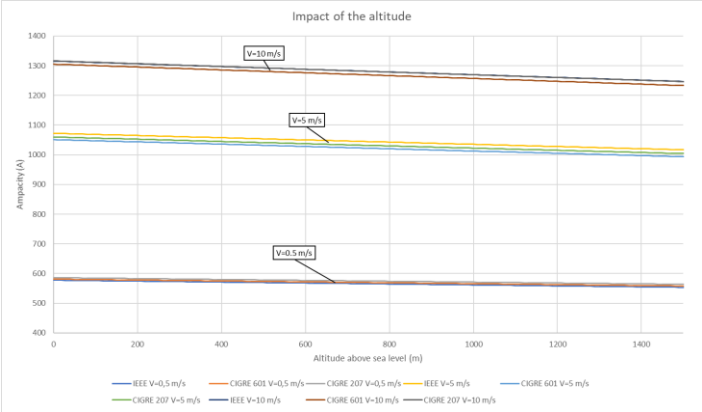

Figure 5: Altitude analysis.

Effectively, the results show that ampacity decreases with increasing altitude having the same weather conditions. As the transmission line elevation rises, the cooling mechanisms, such as convection, become less efficient due to the decrease in air density at higher altitudes. As the altitude parameters embeds the air density parameter in the studied formulas, the line's ability to dissipate heat reduces, leading to a lower ampacity.

The data from the study indicate that the ampacity variations due to altitude are more pronounced at higher wind speeds. This is likely because higher wind speeds enhance convective cooling, and when coupled with the impact of altitude on cooling effectiveness, the ampacity reduction becomes more significant.

According to the Royal Decree 223/2008, the regulation on technical conditions for overhead lines, there are three zones on altitude above the sea level: Zone A (altitude less than 500 meters above sea level), Zone B (altitude between 500 and 1000 meters), and Zone C (altitude above 1000 meters) [25]. The study examined the maximum decrement that can occur in each zone, i.e., the decrement for every 500 meters increases in altitude.

The results revealed that the decrement that occurs in 500 meters (which this is the maximum altitude that can vary in each of the zones) at low wind speeds is around 1.5%, and at high wind speeds, it was around 2%. This difference is minimal, suggesting that it is not necessary to use an atlas for precise altitude and it is acceptable and conservative, to use the higher value of the altitude zone based on regulation on technical conditions for overhead lines encompassing the line's location.

- Impact of the absorptivity and emissivity coefficients

Table 4 show the ampacity values varying the solar absorption and emissivity coefficients with the temperature of service of the cable.

For moderate service temperatures, there is minimal impact on ampacity values, with the change between the two extremes (solar absorption=0.9 and emissivity=0.8) and (solar absorption=0.3 and emissivity=0.2) being 2.79% and 0.12% for Ts=65°C and Ts=50°C, respectively, in the case of IEEE calculations. For higher temperatures, the variation is greater, amounting to 5.34% and 4.14% for Ts=100°C and Ts=80°C, respectively.

On the other hand, when the service temperature is higher, emissivity has a greater impact than solar absorption. The reason for that is that the emissivity coefficient ε, impacts more the power radiated when the difference of temperatures between the cable and the surrounding is greater, as the formula shows:

$$P_{rad} \propto \varepsilon * (T_s - T_a)$$

As a result, as the coefficient of emissivity increases the permissible ampacity rises because the radiated power to the environment also increases. Conversely, when the service temperature is lower (T=40°C) and closer to the ambient temperature, the radiated power has less influence, and solar absorbed power becomes more significant. Hence, as the coefficients increase, the absorption coefficient has a more substantial impact, causing the cable to absorb more solar power and thus reducing the ampacity.

Table 4: Ampacity values (A) varying the solar absorption and emissivity coefficients with different temperature of service using the IEEE standard for ampacity calculation.

		IEEE calculation						
	Solar absorption	**0.9**	**0.8**	**0.7**	**0.6**	**0.5**	**0.4**	**0.3**
	Emissivity	**0.8**	**0.7**	**0.6**	**0.5**	**0.4**	**0.3**	**0.2**
Temperature of Service (°C)	**100**	1122.1	1112.4	1102.5	1092.6	1082.5	1072.4	1062.2
	80	974.0	967.4	960.7	954.1	947.3	940.5	933.7
	65	833.3	829.5	825.6	821.8	817.9	814.0	810.0
	50	646.2	646.1	646.0	645.8	645.7	645.6	645.4
	40	467.1	471.2	475.3	479.4	483.4	487.4	491.3

B. Analysis of the data equipment

- Reliability

The reliability of the equipments for the period studied, March 8th to June 29th, is 91.5% and 63.5% for the Supplier 1 and Supplier 2 respectively. Supplier 2 consistently exhibits lower overall reliability compared to Supplier 1. The reason behind this disparity lies in the characteristics of Supplier 2's system. For Supplier 1, the data points lost primarily correspond to periods when their equipment is not functioning correctly, resulting in downtime. These periods are relatively straightforward to identify, as they are instances when the system is completely inactive. However, for Supplier 2, the situation is more complex. In addition to the periods when the entire equipment is non-operational, this supplier also experiences failures when the vibration sensor does not communicate. Furthermore, the challenge is compounded by instances when there are connectivity issues with the external provider.

It's important to note that during moments when an atmospheric variable is missing whether due to sensor failures or communication problems with the external provider Supplier 2 continues to provide a default rating. However, this default rating is not accurate, as it lacks essential input variables.

- Weather variables comparison

Regarding temperature and solar radiation measurements, Supplier 1 and Open-Meteo data show better agreement than Supplier 2's data. Supplier 2's shows higher values and may be due to its reliance on data from a separate meteorological source, rather than having temperature and solar radiation sensors directly on the transmission line. It is possible that the meteorological station is located in a sunnier area compared to the location where Supplier 1 has its sensors (the tower of the line) and where Open-Meteo's station is placed, which could explain the differences in the recorded data.

As for wind measurements, both Supplier 1 and Supplier 2 have sensors installed, which should ideally provide more reliable data as they are being measurement on-site. However, surprisingly, both suppliers' wind speed data shows very low values, not reaching 3 m/s, raising doubts about the accuracy of their measurements. This brings into question the reliability of the wind data provided by both suppliers. The wind speed taken from Open-Meteo is much higher than both suppliers. Respect both suppliers, Supplier 2 shows higher values than Supplier 1.

- Supplier ampacity value comparison

The Table 5 shows the statical results for the ampacity given by the different providers. The ampacity value provided by the Supplier 2 is consistently greater than the value given by the Supplier 1 in most instances. The reason for that is that, as showed before, Supplier 2 is using higher wind speeds values than Supplier 1 for its calculations, resulting in higher ampacity values.

Table 5: Statistical results of the ampacity values given by both Suppliers

	Ampacity (A)	
	Supplier 1	**Supplier 2**
Average	582.08	623.49
Standard deviation	176.90	304.17
Range	575.50	288.64
Maximum	917.50	743.12
Minimum	342.00	454.48

On the other hand, the ampacity values from Supplier 2 exhibit a wider dispersion around the average, as indicated by the higher standard deviation. But surprisingly, the variation between the maximum and minimum ampacity values is more pronounced in Supplier 1, indicating a greater range of variability in their results.

- Ampacity calculation using Suppliers' input data

a) Supplier 1

The Table 6 displays the percentage difference between our calculations and the values provided by Supplier 1. It should be noted that Supplier 1 adopts the CIGRE 207 standard, which accounts for the minimal deviation observed in their results compared to ours. The persistent difference of 1.19% could potentially be attributed to the application of specific safety coefficients by Supplier 1 in their calculations

Table 6: Difference between the ampacity supplier 1 value and the ampacity calculated by using their input data.

	IEEE	***CIGRE 601***	***CIGRE 201***
Average of the difference	-2.13%	-1.42%	-0.93%

It is noteworthy that all our calculations consistently yield higher ampacity values compared to those provided by Supplier 1. This difference could be attributed to the safety coefficient in their calculations, which may lead to variations in the final results.

b) Supplier 2

Table 7 shows how the ampacities calculated using Supplier 2 weather input data are significantly different and lower than the ampacity provided by the supplier. This might suggest that they are using another calculation method for ampacity. It has been assumed that they use the indirect method, but they could potentially be using the direct method, calculating ampacity through sag or clearance. In [26], it is mentioned that this supplier determines real-time sag data based on conductor vibrations measurement, implying that they use sag for ampacity calculation.

Table 7: Difference between the ampacity supplier 2 value and the ampacity calculated by using their input data.

	IEEE	***CIGRE 601***	***CIGRE 207***
Average of the difference	21.18%	20.49%	21.52%

- Periodicity

Table 8 presents the results of the time (minutes) when the ampacity rating calculations for three different scenarios: providing the rating every 15 minutes, 30 minutes, and 1 hour, exceeds the real- time ampacity. The calculations were performed using three methods: taking the average of minute-by-minute ratings from the preceding time period, using the most restrictive ampacity value from the preceding time period, and presenting the instantaneous real-time rating for each time.

When the average ampacity rating from the preceding period is considered, the highest average values are observed for the 1-hour scenario, followed by the 30-minute scenario and the 15-minute scenario. However, the differences are not very high, as it is the average time of each of the periods that the given ampacity exceed the real one, but it does not account for how many times occurs. It is evident that in the case of given the minimum value from the preceding period reduces the times that it occurs.

The median time duration, in almost all cases, is 2 minutes. This means that the cable is able to withstand these durations without the calculated ampacity exceeding the real-time ampacity.

The critical time periods occur when the ampacity starts to decrease for extended durations. In such cases, providing the value of the average of the preceding period, the minimum value, or the instantaneous value would still result in a higher ampacity rating than that of the subsequent period, as the ampacity is decreasing.

In this scenario of decreasing ampacity, combining on-site measurements with forecasted data can be effective in anticipating ampacity decreases. It's possible to select the lower ampacity value calculated from both on-site measurements and forecasts. Another approach is to apply a safety factor to the calculated ampacity when a decrease is detected between periods, reducing the duration during which the given ampacity exceeds the actual one.

- Emissivity and solar absorption coefficients

Having understood the variation of ampacity with coefficients, this knowledge is applied to our study line. The conductor coefficients for this line are: Solar Absorption=0.6 and Emissivity=0.5, with a service temperature of 65°C. The ampacity value has been calculated for a full day using both the actual coefficients of the line and the coefficients recommended by IEEE (Solar Absorption=0.7, Emissivity=0.6) and CIGRE 601 (solar absorption=0.8, emissivity=0.7). The Table 9 displays the absolute variation in ampacity when comparing the results with the calculation using the actual coefficients. Notably, the variations are more significant when using the coefficients recommended by IEEE compared to the recommendations of CIGRE 601. This discrepancy arises because the coefficients recommended by IEEE differ more from the actual coefficients of our study line.

Table 9: Comparison of ampacity values using default and actual coefficients - Average absolute difference.

	IEEE	***CIGRE 601***	***CIGRE 207***
Solar absorption=0.7 Emissivity=0.6 (CIGRE 601 recommendation)	2.18%	2.10%	**2.09%**
Solar absorption=0.8 Emissivity=0.7 (IEEE recommendation)	**4.30%**	4.14%	4.12%

- Solar radiation

The Figure 6 shows solar radiation throughout the entire day. It depicts the solar radiation measured by the sensor (Qsensor), the solar radiation estimated using the IEEE formula (Q1), the solar radiation estimated using the CIGRE 601 formula (Q2), the solar radiation predicted by Open-Meteo (Q3), and finally, the radiation estimated based on historical maximum radiation (Q4).

As observed, the largest difference in solar radiation lies with Q1 and Q2, which are the estimated values based on standards. The predicted values, Q3, and the values estimated based on the maximum solar radiation, Q4, resemble the real values more closely.

Table 8: Statistics of the time in minutes when the ampacity given different frequencies (15 min, 39 min, and 1 hour) exceeds the real-time ampacity.

	15 MIN			***30 MIN***			***1 HOUR***		
	Average	**Minimum**	**Instantaneous**	**Average**	**Minimum**	**Instantaneous**	**Average**	**Minimum**	**Instantaneous**
Average	4.92	2.79	4.66	5.68	3.31	4.94	6.44	3.68	5.93
Maximum	140	14	14	141	29	29	144	57	59
Median	2	1	1	2	2	2	2	2	2

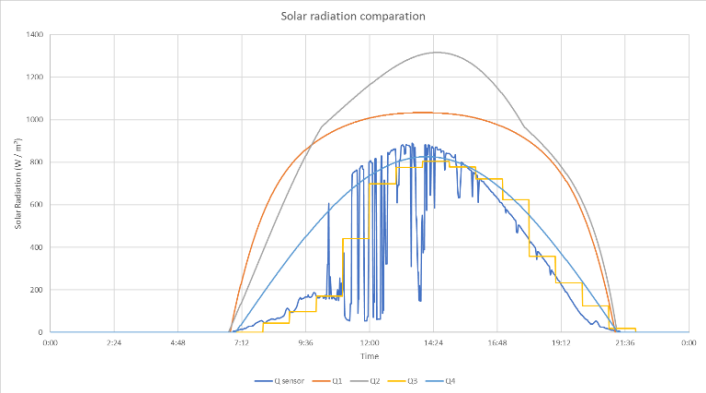

Figure 6: Solar radiation estimated by different ways and Solar radiation measured with the sensor.

The Table 10 presents the absolute percentage difference between the estimated and the measure solar radiation values, as well as the variation in the final ampacity calculation when using the sensor's measurement and the estimated values. Although there is a considerable difference between the estimated values and the measurement of solar radiation, its influence on the ampacity calculation is not significant.

Table 10: Absolute percentage difference between the estimated and the measure solar radiation values.

	Q1	***Q2***	***Q3***	***Q4***
Solar radiation variation	255.95%	252.79%	52.04%	93.28%
Ampacity variation	4.25%	6.30%	0.93%	1.57%

Among the different estimated solar radiation values (Q1, Q2, Q3, and Q4), Q3, which represents the solar radiation predicted, exhibits the least variation. Specifically, the variation in Q3 is 52.04% compared to the actual measured solar radiation and the ampacity calculation using Q3 as an input show only a 0.93% variation compared to the calculation based on the actual measured solar radiation.

- Simplified wind calculation

When implying the proposed simplifications:

Simplification 1:

- $\text{Day} + \text{Wind speed} \geq \frac{15\text{km}}{\text{h}} \rightarrow \text{YES wind} \rightarrow$ Wind speed for formula: $\frac{1.2\text{m}}{\text{s}}$.
- $\text{Day} + \text{Wind speed} < \frac{15\text{km}}{\text{h}} \rightarrow \text{NO wind} \rightarrow$ Wind speed for formula: 0.6m/s.
- $\text{Night} \rightarrow \text{NO wind} \rightarrow$ Wind speed for formula: 0.6m/s.
- Wind direction $= 15°$.

Simplification 2:

- $\text{Day} + \text{Wind speed} \geq \frac{9.36\text{ km}}{\text{h}} \rightarrow \text{YES wind} \rightarrow$ Wind speed for formula: $\frac{1.2\text{m}}{\text{s}}$.
- $\text{Day} + \text{Wind speed} < \frac{9.36\text{ km}}{\text{h}} \rightarrow \text{NO wind} \rightarrow$ Wind speed for formula: 0.2m/s.
- $\text{Night} \rightarrow \text{NO wind} \rightarrow$ Wind speed for formula: 0.2m/s.
- Wind direction $= 90°$.

Both suppliers consistently fall under the no-wind condition (0.6 m/s and 0.2 m/s in simplifications 1 and 2, respectively) since the limit is never exceeded at any time. This is because the measurements from Supplier 1 and Supplier 2 are strangely very low at all times, as said before.

Respect the ampacity values calculated with these simplifications: the simplified wind approach manages to smooth out the curve of both suppliers, but during the night, the ampacity value given exceeds the real value. This could be because the assumed wind data during the night in the simplifications is relatively higher compared to the one that the sensor measures, although in reality, 0.6 m/s is considered a light breeze. The problem might indeed lie in the measurement of wind data by both suppliers, which consistently appears very low.

On the other hand, when using the simplifications with the wind values from the historical data, these simplifications work better as the wind values are higher and surpasses the threshold. The conservative values assumed in both simplifications ensure that ampacity calculations are carried out with caution. This approach helps maintain safety margins and ensures that the calculated ampacity values are not underestimated, even in the presence of more severe wind conditions. Simplification 2 tends to align more closely with the ampacity calculated using the non-simplified wind data, as Table 11 shows.

Table 11: Absolute differences between the simplified and non-simplified approaches.

	Supplier 1		***Supplier 2***		***Historical data***	
	Simplification 1	**Simplification 2**	**Simplification 1**	**Simplification 2**	**Simplification 1**	**Simplification 2**
Wind speed difference (m/s)	0.13	0.37	0.76	1.16	2.75	2.79
Ampacity difference (%)	12.60%	12.73%	33.67%	33.92%	45.20%	35.52%

- Ambient temperature analysis

For this section, meteorological data from Supplier 1 and the prediction from Open Meteo is used. Two days are selected—one with low temperatures on 24th January 2023 and another with high temperatures on 25th June—to study both extremes. The ampacity calculations follow the IEEE standard.

Two cases are considered for the ambient temperature used in the ampacity calculation:

1. Taking the predicted temperature and multiplying it by a safety factor based on the distance to the point being calculated (K=1.1 by default during the day, K=1 by default during the night).
2. Considering the maximum value among the current temperature measured by the sensor of Supplier 1, and the prediction.

Table 12 and Table 13 show the difference between the methods with parametrized temperatures and the case of non-parametrized temperatures, i.e., using directly temperatures measured by the sensor, for the day with high and low temperatures, respectively.

Table 12: Differences between the parameterized methods and the non-parametrized one for the day with high temperatures.

	Predicted*Coefficient	***Maximum***
Temperatures difference (°C)	1.20	1.28
Ampacity difference (%)	1.5%	1.1%

Table 13: Differences between the parameterized methods and the non-parametrized one for the day with low temperatures.

	Predicted*Coefficient	***Maximum***
Temperatures difference (°C)	2.81	1.40
Ampacity difference (%)	4.4%	1.81%

The analysis confirms that both methods of temperature consideration, either using the predicted temperature with a coefficient or selecting the higher temperature value, result in relatively small differences in ampacity calculations. Additionally, it is confirmed that in the case of using the predicted temperature multiplied by coefficients, which would be applicable when a temperature sensor is not available, the chosen coefficients provide a safe and reliable estimation.

VIII. Conclusions

In summary, implementing Dynamic Line Rating (DLR) across an entire network like that of Iberdrola entails a significant journey that must be well studied as it presents both opportunities and challenges. Many studies have shown that power line capacity can be improved through DLR, but in order to implement it on a large scale, critical issues of reliability, security and data accuracy need to be addressed. Iberdrola's initial step has been to deploy pilot equipment from different suppliers on selected lines. This project has focused on analysing the data from this equipment, with the future perspective of using DLR as input data for the Optimal Power Flow (OPF), to improve the flexibility of the grid.

Multiple conclusions are drawn from the analyses performed. DLR offers an alternative to grid reinforcement, as it is a solution that can be quickly adopted. However, the installed pilot equipment is not very reliable. In addition, both suppliers consistently measure very low wind speed values, which leads to uncertainty about the accuracy of the measurements.

As the ampacity calculated using the suppliers' input variables is not equal to the ampacity reported by them, it may mean undisclosed coefficients or simplifications. It is necessary to engage in dialogue with suppliers to address reliability concerns, verify measurement accuracy, and acquire vital information on calculation methodologies.

Solar radiation and ambient temperature do not require on-site measurements, as estimations and predictions provide accuracy values. On the other hand, the need for wind measurements should be evaluated for potential placement on all lines or just critical ones. Conductor temperature sensor is not necessary, but it can be used to verify that the measured cable temperature corresponds to the expected ampacity result.

In conclusion, it is necessary to have reliable equipment, to choose which measurement strategy is suitable and to use predicted data, as variations in ampacity can be forecast. It is necessary to assess the desired periodicity, as it has to be a safe value, and it also has to serve as input data for the OPF. These synthesised conclusions provide recommendations to guide Iberdrola in the formulation of a comprehensive deployment plan for 2030.

References

[1] 'Acuerdo de París sobre el Cambio Climático', Feb. 03, 2023. https://www.consilium.europa.eu/es/policies/climate-change/paris-agreement/ (accessed Jun. 19, 2023).

[2] 'EUniversal_D1.3_Challenges-and-opportunities-for-electricity-grids-and-markets.pdf'. Accessed: Aug. 12, 2023. [Online]. Available: https://euniversal.eu/wp-content/uploads/2021/08/EUniversal_D1.3_Challenges-and-opportunities-for-electricity-grids-and-markets.pdf

[3] 'Las energías renovables podrían alcanzar el 50% del "mix" de generación eléctrica en España en 2023 | Red Eléctrica'. https://www.ree.es/es/sala-de-prensa/actualidad/nota-de-prensa/2023/03/las-energias-renovables-podrian-alcanzar-50porciento-del-mix-de-generacion-electrica-en-espana-en-2023 (accessed May 25, 2023).

[4] R. Mínguez, R. Martínez, M. Manana, A. Arroyo, R. Domingo, and A. Laso, 'Dynamic management in overhead lines: A successful case of reducing restrictions in renewable energy sources integration', *Electr. Power Syst. Res.*, vol. 173, pp. 135–142, Aug. 2019, doi: 10.1016/j.epsr.2019.03.023.

[5] L. Rácz, G. Gabor, and B. Németh, 'Different Approaches of Dynamic Line Rating Calculations', in *2019 7th International Youth Conference on Energy (IYCE)*, Jul. 2019, pp. 1–6. doi: 10.1109/IYCE45807.2019.8991570.

[6] 'Repotenciación: la gran renovación del parque renovable en España', *El Periódico de la Energía*, Mar. 21, 2023. https://elperiodicodelaenergia.com/repotenciacion-la-gran-renovacion-del-parque-renovable-en-espana/ (accessed May 29, 2023).

[7] A. Sendin, J. Matanza, and R. Ferrús, *Smart Grid Telecommunications: Fundamentals and Technologies in the 5G Era*. Hoboken, NJ, 2021.

[8] R. Martínez, A. Arroyo, M. Mañana, P. Bernardo, R. Mínguez, and R. Garrote, 'A comparison of different methodologies for rating definition in

overhead lines', *Renew. Energy Power Qual. J.*, pp. 806–810, May 2016, doi: 10.24084/repqj14.470.

[9] T. Song and J. Teh, 'Dynamic thermal line rating model of conductor based on prediction of meteorological parameters', *Electr. Power Syst. Res.*, vol. 224, p. 109726, Nov. 2023, doi: 10.1016/j.epsr.2023.109726.

[10] M. Simms and L. Meegahapola, 'Comparative analysis of dynamic line rating models and feasibility to minimise energy losses in wind rich power networks', *Energy Convers. Manag.*, vol. 75, pp. 11–20, Nov. 2013, doi: 10.1016/j.enconman.2013.06.003.

[11] D. J. Spoor and J. P. Roberts, 'Development and experimental validation of a weather-based dynamic line rating system', in *2011 IEEE PES Innovative Smart Grid Technologies*, Nov. 2011, pp. 1–7. doi: 10.1109/ISGT-Asia.2011.6257099.

[12] T. Yip, C. An, G. Lloyd, M. Aten, and B. Ferri, 'Dynamic line rating protection for wind farm connections', in *2009 CIGRE/IEEE PES Joint Symposium Integration of Wide-Scale Renewable Resources Into the Power Delivery System*, Jul. 2009, pp. 1–5.

[13] C. A. E. Realpe, 'Using the concept of dynamic line rating to facilitate the integration of variable renewable energy and to optimize the expansion of the German power grid'.

[14] S. Karimi, P. Musilek, and A. M. Knight, 'Dynamic thermal rating of transmission lines: A review', *Renew. Sustain. Energy Rev.*, vol. 91, pp. 600–612, Aug. 2018, doi: 10.1016/j.rser.2018.04.001.

[15] D. Hardman, N. Murdoch, and J. Berry, 'THE BENEFITS AND DESIGN OF A DYNAMIC PROTECTION SYSTEM FOR THE DISTRIBUTION NETWORK', 2019.

[16] 'Dynamic Line Rating: Innovation Landscape Brief'.

[17] 'Congressional_DLR_Report_June2019_final_508_0.pdf'. Accessed: May 29, 2023. [Online]. Available: https://www.energy.gov/sites/prod/files/2019/08/f66/Congressional_DLR_Report_June2019_final_508_0.pdf

[18] 'Guide for thermal rating calculations of overhead lines', *e-cigre*. https://e-cigre.org/publication/601-guide-for-thermal-rating-calculations-of-overhead-lines (accessed May 25, 2023).

[19] 'IEEE Standard for Calculating the Current-Temperature Relationship of Bare Overhead Conductors', *IEEE Std 738-2012 Revis. IEEE Std 738-2006 - Inc. IEEE Std 738-2012 Cor 1-2013*, pp. 1–72, Dec. 2013, doi: 10.1109/IEEESTD.2013.6692858.

[20] A. Arroyo *et al.*, 'Comparison between IEEE and CIGRE Thermal Behaviour Standards and Measured Temperature on a 132-kV Overhead Power Line', *Energies*, vol. 8, no. 12, Art. no. 12, Dec. 2015, doi: 10.3390/en81212391.

[21] S. Abbott, S. Abdelkader, L. Bryans, and D. Flynn, 'Experimental validation and comparison of IEEE and CIGRE dynamic line models', in *45th International Universities Power Engineering Conference UPEC2010*, Aug. 2010, pp. 1–5.

[22] F. Gómez, J. M. De María, D. Puertas, A. Baïri, and R. Granizo, 'Numerical study of the thermal behaviour of bare overhead conductors in electrical power lines', Jan. 2011.

[23] I. A. S. Rincón, 'Análisis de Metodologías Para el Cálculo de la Ampacidad en Conductores Desnudos'.

[24] ' Free Open-Source Weather API | Open-Meteo.com'. https://open-meteo.com/ (accessed Aug. 01, 2023).

[25] 'Machine Translation of "Royal Decree 223/2008 Of 15 February, Laying Down The Regulations On Technical Conditions And Guarantees Of Security In ..." (Spain)'. https://www.global-regulation.com/translation/spain/1444584/royal-decree-223-2008-of-15-february%252c-laying-down-the-regulations-on-technical-conditions-and-guarantees-of-security-in-high-voltage-power-lines-and.html (accessed Aug. 02, 2023).

[26] K. Morozovska and P. Hilber, 'Study of the Monitoring Systems for Dynamic Line Rating', *Energy Procedia*, vol. 105, pp. 2557–2562, May 2017, doi: 10.1016/j.egypro.2017.03.735.